Experimental Error Performance of Modulation Schemes Under a Controlled Laboratory Turbulence FSO Channel

Rajbhandari, S. , Ghassemlooy, Z. , Haigh, P. A. , Kanesan, T. and Tang, X.

Original citation & hyperlink:
Rajbhandari, S. , Ghassemlooy, Z. , Haigh, P. A. , Kanesan, T. and Tang, X. (2015) Experimental Error Performance of Modulation Schemes Under a Controlled Laboratory Turbulence FSO Channel. Journal of Lightwave Technology, volume 33 (1): 244 – 250
http://dx.doi.org/10.1109/JLT.2014.2304182

ISSN 0733-8724
DOI 10.1109/JLT.2014.2377155

Experimental Error Performance of Modulation Schemes under a Controlled Laboratory Turbulence FSO Channel

Sujan Rajbhandari, *Member IEEE*, Zabih Ghassemlooy, *Senior Member IEEE*, Paul Anthony Haigh, *Member IEEE*, Thavamaran Kanesan, *Member IEEE*, and Xuan Tang

***Abstract*—This paper experimentally investigates the performance of different modulation schemes under the atmospheric turbulence conditions for free space optical communication links. The experiments were carried out in a dedicated and controlled indoor atmospheric chamber. The turbulence environment was created by introducing hot air, while the temperature profile was monitored throughout the chamber to maintain a constant environment. By evaluating the error performance of different modulation schemes under identical conditions, it was observed that pulse position modulation offers the best performance, followed by subcarrier intensity modulation under weak turbulence environments.**

***Index Terms*— Free space optics, turbulence, modulation schemes, bit error rate**

I. INTRODUCTION

THERE HAS BEEN significant interest in terrestrial free space optics (FSO) communication technology over the last decade for future wireless access networks for a range of applications. This is mostly due to exponential growth in data traffic, resulting in significant bandwidth congestion in the radio frequency (RF) based technologies; in particular the last mile access bottleneck [1, 2]. Recent forecasts indicate that service providers will find it challenging to meet the high demand for access to wireless data without investment in new technologies or acquisition of new frequency spectra at a premium cost. FSO technology can address the looming bandwidth shortage in certain applications. FSO systems offer license free wide spectra, inherent security, no electromagnetic interference with RF, compatibility with the optical fibre back-bone network infrastructure and relatively low capital and operating costs. The deployment of FSO systems is particularly advantageous in metropolitan areas, geographically challenging terrains and under-served rural areas lacking broadband network connectivity. In such areas, the installation of optical-fibre links are the least feasible or impossible, as evident from the numerous case studies brought forward by FSO suppliers. Current last mile access networks, particularly in urban areas, are largely based on RF technologies which offer far lower capacity than the back bone network. Nevertheless, with exponentially increasing data traffic, it is inevitable that an alternative technology is sought-after and FSO is one of the most promising technologies for such application [2].

As with all wireless systems, FSO links are susceptible to ever-changing environmental conditions. Fog, smoke and rain can result in large attenuation. For instance; dense fog can result in attenuation > 270 dB/km, thus limiting the link length to less than few hundred meters [2]. Another key challenge in FSO systems is the phenomenon of fading due to scintillation [3]. The random fluctuation in temperature and pressure in the atmosphere results in indiscriminate variations of the refractive indices of air. Such intensity fluctuations, also known as scintillation, can dramatically degrade the performance of intensity modulation with direct detection (IM/DD) FSO links. even in clear weather conditions, as is evident from both the experimental and the analytical results in [4].

The goal of this study is to experimentally compare and establish an appropriate modulation scheme for FSO systems in the turbulent environment for the first time. Both baseband and subcarrier based modulation schemes have previously been adopted in FSO systems [5, 6]. Baseband on-off keying (OOK) is the most common method used in many commercially available FSO systems due to its simplicity and low implementation cost. In an additive white Gaussian noise channel (AWGN), the optimum OOK receiver uses a threshold detector with a fixed threshold level at the output of a matched filter. OOK based FSO links employing a fixed threshold level at the receiver are very susceptible to high bit errors under the turbulence regime due to fluctuations of the

Manuscript received April, 2014.

Sujan Rajbhandari is with the Department of Engineering Science, University of Oxford, Oxford, UK. E-mail: sujan@ieee.org.

Z. Ghassemlooy are with the Optical Communications Research Group, Faculty of Engineering and Environment, Northumbria University, Newcastle, NE1 8ST, UK. E-mail: z.ghassemlooy@northumbria.ac.uk,

P. A. Haigh is with the Department of Electronic and Electrical Engineering, University College London, WC1E 6BT, UK. He is also with Faculty of Electromagnetic Field, Czech Technical University in Prague, technicka 2, 166 27 Prague 6, E-mail: paul.anthony.haigh@ieee.org

T. Kanesan is with Telekom Research & Development (TM R&D), TM Innovation Centre, 63000 Cyberjaya, Selangor, Malaysia, e-mail: thavamaran.kanesan@ieee.org.

X Tang is with Fujian Institute of Research on the Structure of Matter, Chinese Academy of Sciences, Fujian, China, Email: xtang@fjirsm.ac.cn.

received optical power. In such conditions, employing an adaptive threshold detector would improve the link performance at the cost of complex implementation [5, 7]. However, the adaptive thresholding requires the continuous monitoring and the knowledge of channel state in order to which makes it difficult to implement in the practical system.

Pulse position modulation (PPM), where information is encoded into the position of the optical pulse rather than amplitude, offers higher resilience to turbulence due to the availability of soft demodulation algorithms [8]. Alternatively, one could adopt subcarrier intensity modulation (SIM) schemes by modulating the frequency and phase of the RF carrier [5, 6]. The phase fluctuation is less pronounced in turbulent channels and hence SIM offers improved performance over OOK. Under strong turbulence regimes, one could combine the best of both worlds by merging PPM and SIM in order to improve the FSO link performance. In [9], it has been shown that a hybrid PPM-SIM scheme offers enhanced link performance in comparison to SIM in a strong turbulence regime.

In the literature there are a large number of papers showing a theoretical analysis of these modulation schemes [5, 6, 10, 11], but there are very few comprehensive experimental studies to compare their performance in a turbulent channel and hence it is imperative such a study is reported. The objective of this paper is to address this imbalance between theory and practice by developing a platform for further comprehensive studies of the FSO link employing different modulation schemes. In practice, FSO link assessment highly depends on gathering measured signal data over a long period of time in an outdoor environment. Thus, being able to ensure identical test conditions for all schemes is effectively impossible. The time and cost involved in such a process explains the lack of real-life data published in the literature. Hence, practical investigations are carried out using a dedicated indoor testbed under a controlled environment, closely mimicking outdoor conditions [12]. The key advantage of the indoor testbed (i.e. the atmospheric chamber) is the ability to quickly carry out a large number of measurements under various environmental conditions, something that would take a very long time in the outdoor environment. In previous works, it has been established that the received optical intensity within the chamber in the presence of turbulence follows the log-normal profile; which is consistent with observations of the outdoor environment; thus validating the measurements within the chamber [12]. This paper presents a slot error rate (SER) performance comparison between different modulation schemes for FSO systems in a turbulence channel.

The rest of the paper is organized as follows: Section II introduces the modulation schemes and experimental set-up. The experimental set-up parameters are also summarized in this section. Section III reports the experimental error performances of the modulation schemes under different turbulence strengths. Finally, the concluding remarks are drawn in Section IV.

II. Experimental Set-up

A. Modulation Schemes

OOK is the dominant modulation scheme in commercial terrestrial FSO systems. This is primarily due to its simplicity and resilience to the innate nonlinearities of the laser and/or external modulator. In OOK, an optical pulse of peak power P_t represents the digital symbol '1' and absence of a pulse represent the digital symbol '0'. The optical pulse occupies the whole bit duration T_b in non-return-to-zero (NRZ) format and a fraction of the bit duration in return-to-zero (RZ). Hence, the average transmitted power for OOK-NRZ is $P_t/2$. PPM is an orthogonal modulation technique, in which a block of $\log_2 L$ data bits are mapped onto one of L possible symbols. Each symbol consists of a pulse of constant power P_t occupying one slot, along with (L-1) empty slots. The position of the pulse within a symbol corresponds to the decimal value of the $\log_2 L$ data bits. PPM is substantially more power efficient than OOK at the cost of an increased bandwidth requirement and greater complexity. To achieve the same data rate as OOK, the required slot duration T_{s_ppm} of PPM is [2]:

$$T_{s\_ppm} = \frac{T_b \log_2 L}{L} \tag{1}$$

Similar to OOK; PPM symbols can be 'hard' decoded using a matched filter followed by a simpler threshold detector. As the probabilities of receiving '0' and '1' are not equal (probability of receiving '0' is (L-1) times higher than receiving '1' in PPM), the optimum threshold level for hard decision decoding (HDD) does not normally lie midway between '1' and '0' levels but can be easily calculated. Alternatively, one could use the 'soft' decision decoding (SDD) scheme, which is optimal for decoding PPM symbols. In this approach, a block of L-sample is passed to a SDD, which assigns a '1' to the slot containing the sample of largest amplitude and '0' to the remaining slots. Since the relative amplitude (not the absolute amplitude) of the pulse within a slot in a symbol is of prime importance in SDD, then SDD can be considered optimal in a turbulence channel.

In the SIM technique, borrowed from the very successful multiple carrier RF communications, a number of baseband digital signals are frequency up-converted prior to intensity, frequency, or phase modulation of the optical carrier. Orthogonal frequency division multiplexing (OFDM) is a special case of multi-carrier SIM in which carriers are orthogonally spaced, thus offering higher spectral efficiency. The main drawback of IM/DD based SIM is its poor optical average power efficiency and a high peak-to-average power ratio (PAPR) [2]. Since the electrical SIM signal has both positive and negative values, then inclusion of a DC bias is needed to satisfy the requirement for non-negative optical intensity. As an example, in non-distorting channels with IM/DD and AWGN, binary phase-shift keying (BPSK) and quadrature phase-shift keying (QPSK) both require and additional 1.5 dB optical power in comparison to OOK. During one symbol duration, the SIM symbol $m(t)$ is given by [2]:

Fig. 1 Block diagram of the laboratory turbulence chamber

$$m(t) = \sum_{i=1}^{N_s} g(t)a_{ic}\cos(\omega_{ci}t + \varphi_i) + g(t)a_{is}\sin(\omega_{ci}t + \varphi_i) \quad (2)$$

where N_s is the number of subcarriers, $g(t)$ is the pulse shape function, $[\omega_{ci}, \varphi_i]_{i=1}^{N}$ is the angular frequency and phase and $\{a_{ic}, a_{is}\}_{i=1}^{N}$ corresponds to the constellation in use.

An appropriate DC level is added to $m(t)$ before IM of the optical source. The transmitted power is defined as:

$$P_t(t) = P[1 + \xi m(t)] \quad (3)$$

where P is the average transmit optical power of the laser beam and ξ is the modulation index that satisfies the $-1 < \xi m(t) < 1$ condition in order to avoid overmodulation. Note that one advantage of SIM is that one could use a range of modulation techniques for $m(t)$. The received electrical signal in the absence of distortion can be modelled as:

$$i(t) = RI[1 + \xi m(t)] + n(t) \quad (3)$$

where R is photodetector (PD) responsivity, I is the instantaneous optical irradiance, and $n(t)$ is the AWGN with zero mean and variance σ_n^2. This is followed by a standard RF demodulator to recover the transmitted symbols; details of which can be found in [2].

The hybrid version of PPM and SIM is similar to the SIM scheme described above except that the modulation scheme is baseband PPM [9]. Since SDD is also possible in PPM-SIM, in [9] it has been shown that PPM-SIM outperforms SIM in the presence of turbulence.

B. Experimental Set-up

The experimental set-up for the measurements is depicted in Fig. 1. A 2^{11}-1 pseudorandom bit sequence (PRBS-11) is generated and encoded into the desired modulation format using MATLAB. These signals are then loaded into the Tektronix AFG3252 arbitrary waveform generator, which modulates the laser source with a narrow diverged beam at an operating wavelength of 830 nm. The transmitted optical power is controlled externally using neutral density filters placed close to the laser. The IM optical signal is transmitted through the indoor FSO chamber before being collected at the receiver. The FSO chamber is a closed glass chamber with a dimension of 5.50 × 0.30 × 0.30 m^3. There are a number of vents for hot and cold air circulation. The temperature within the chamber is controlled by external fans, which blow cold/hot air perpendicular to the propagating laser beam. There are 11 thermal sensors spaced evenly at every 0.50 m along the chamber, which are used to obtain the temperature profile. The temperature sensors located along the chamber are sampled at interval of 67 ms. In order to establish identical operating conditions for all modulation schemes; the temperature profile throughout the chamber is maintained constant. The strength of the turbulence was varied by means of controlling the output of the hot and cold fan heaters (i.e. varying the temperature profile). All the key system parameters adopted for the experimental set-up are given in Table I.

The received signal is then digitized using an Agilent DSO9254A real time oscilloscope, and then transferred to a PC for further processing. The symbol synchronization, matched filtering and symbol decoding are all carried out in MATLAB. For both OOK and PPM, mid-point sampling is adopted followed by threshold decoding and SDD schemes. For BPSK and PPM-BPSK, the standard RF demodulator is utilized to recover the transmitted symbol. The recovered sequence is then compared with the transmitted sequence symbol-by-symbol to measure the slot (bit) error probability. The link performance is also measured using the Q-factor, which is defined as [14]:

$$Q = \frac{v_H - v_L}{\sigma_H + \sigma_L} \quad (4)$$

where v_H and v_L are the mean received voltages and σ_H and σ_L are the standard deviations for the '1' and '0' levels, respectively.

The received signal at the receiver output can be described by the conventional channel model:

$$y_\kappa = hRx_\kappa + n_o \quad (6)$$

where h is the channel state, x_κ is the optical intensity of the transmitted signal and n_o is signal-independent AWGN. The channel state $h = h_{a\text{-}t}h_{a\text{-}gp}$ where $h_{a\text{-}t}$ and $h_{a\text{-}gp}$ are the attenuation due to the atmospheric turbulence, and geometric spread and pointing errors, respectively.

TABLE I
PARAMETERS OF THE FSO LINK

Parameters		Values
Data Source	Data rate, R_b	1 Mbps
	Modulation	NRZ, PPM, BPSK, PPM-BPSK
	Bit resolution, L	2,4
Laser diode	Peak wavelength	830 nm
	Maximum optical power	10 mW
	Beam size at aperture	5 mm × 2 mm
	Beam divergence	5 mrad
	Modulation bandwidth	75 MHz
Channel	Dimension	5.50 × 0.30 × 30 m^3
	Rytov variance	< 0.23
Receiver	PD absorption range	750 - 1100 nm
	PD active area	1 mm^2
	PD responsivity R	0.59 A/W at 830 nm
	Bandwidth	120 MHz

In FSO systems, the strength of turbulence is characterized by the normalized variance (i.e. scintillation index (SI)) σ_I^2 defined as [15]:

$$\sigma_I^2 = \frac{\langle I^2 \rangle}{\langle I \rangle^2} - 1 \tag{5}$$

where $\langle . \rangle$ denotes the ensemble average equivalent to long-time averaging with the assumption of an ergodic process. For the weak turbulence regime ($\sigma_I^2 < 1$), the SI is commonly distinguished through the values of Rytov variance, which is defined as [15]:

$$\sigma_x^2 = 0.56k^{7/6} \int_0^{L_p} C_n^2(x)\left(L_p - x\right)^{5/6} dx \tag{6}$$

where C_n^2 is the refractive index structure parameter with a typical range from 10^{-17} $\mathrm{m}^{-2/3}$ for weak turbulence regime and up to 10^{-13} $\mathrm{m}^{-2/3}$ for the strong turbulence regime ($(\sigma_I^2 \gg 1)$, L_P is the propagation length, $k = 2\pi/\lambda$ is the spatial wave number and λ is the operating wavelength (830 nm in this case).

The refractive index structure parameter C_n^2 is highly dependent on the small scale temperature fluctuation, the temperature structure constant C_T^2 and the atmospheric pressure *P*, which is given by [15]:

$$C_n^2 = \left(86 \times 10^{-6} \frac{P}{T^2}\right)^2 C_T^2 \text{ for } \lambda = 850 \text{ nm} \tag{7}$$

For a plane wave,$\sigma_I^2 = 4\sigma_x^2$. The maximum temperature achieved in the chamber was 60°C. Assuming a constant temperature gradient, the maximum achievable σ_I^2 is 0.9 (< 1). The distribution of amplitude fluctuation can be approximated by the log-normal distribution. Thus, the probability density function (PDF) of the received irradiance *I* due to the turbulence is derived by [16]:

$$P(I) = \frac{1}{\sqrt{2\pi\sigma_I^2}} \frac{1}{I} \exp\left\{ - \frac{\left(\ln\left(I/I_0\right) + \sigma_I^2/2\right)^2}{2\sigma_I^2} \right\} \tag{8}$$

where I_0 is the irradiance when there is no turbulence in the channel.

For an AWGN channel without fading and distortion, the received electrical signal-to-noise ratio (SNR_0) is defined as [17]:

$$SNR_0 = \frac{(RP_r\xi)^2}{\sigma_n^2} \; ; \tag{9}$$

where P_r is the average received optical power.

In the presence of turbulence, the instantaneous irradiance experiences fluctuations, thus leading to the variation in instantaneous SNR. In the lognormal fading channel, the ensemble mean of SNR can be expressed as [18]:

$$\langle \mathrm{SNR} \rangle = \frac{\mathrm{SNR}_0}{\sqrt{\sigma_I^2 (\mathrm{SNR}_0)^2 + I_0/\langle I \rangle}}. \tag{10}$$

The error probability for a given modulation format is a function of SNR and SI. The closed form expressions for the error probability for different modulation schemes are derived in [2, 9]. From (7-9), in order to maintain the SI level, the temperature profile C_T^2 needs to be regulated. In our experimental set-up, the temperature profile is regulated and constantly recorded. The SI is then calculated from the temperature profile using (8) and (9), or measured using the received optical intensity (7). In [12] it is shown that both measured and predicted SI parameters using (7) and (8), respectively agree well, thus validating the experimental results. Since experimentally obtained $\sigma_I^2 < 0.9$, then the PDF of the received optical irradiance closely follows the log-normal distribution defined by (10). The details of the measured intensity distribution in the presence of turbulence is given in [12] and hence it is not replicated here. Adopting these predicted results, we can estimate the SNR for a given SI using (11) and (12) as well as determine the error probability. The derivation of the close form error estimation is beyond the scope of this paper. Interested readers can refer to [2, 9] and the references therein.

III. Results and Discussion

In order to establish the error performance of the link, a PRBS-11 was generated and encoded to the appropriate modulation format, which was then transmitted through the channel as mentioned above. Even though system bandwidth was 75 MHz (limited mainly by the laser bandwidth), the operating data rate is set to 1 Mbps for the following reasons: (*i*) the objective of the experiment was not to set a record data rate, rather to compare different modulation schemes in identical environmental conditions, and (*ii*) low data rates allowed us to monitor the channel effects for an increased time duration for any given number of transmitted symbols. In the experimental set-up at least 50 MSyms were processed for each modulation scheme, corresponding to a 50 s time frame at 1 Mbps. Experiments were repeated at least three times at different times to ensure validation of the results, which effectively makes the total number of slot analyzed equal to 150 MSyms. Data rates lower than 1 Mbps are not feasible as the baseline wander effect becomes prevalent in OOK, rendering the test unfair since this effect is not common across the modulation schemes under test [19].

For SIM, the carrier frequency is set at twice the slot rate. In order to achieve the same data rate as OOK, the slot rate for PPM and PPM-BPSK is 2 Mslot/s (refer to (1)). The average transmitted optical power for OOK, 2-PPM, BPSK and 2, 4-PPM-BPSK was made equal. This was achieved by setting equal peak optical power, which is controlled by the peak-to-peak voltage of the electrical signal. The average transmitted optical power of 4-PPM was set to half that of the other modulation schemes to make the peak optical power equal for all the modulation schemes. This is to provide a fair comparison across the modulation schemes. In order to keep the same average optical power, 4-PPM requires higher peak-to-peak voltage (which corresponds to higher peak optical power). Hence, 4-PPM will provide a higher *Q*-factor in the absence of turbulence, leading to lower SER. This can give an unfair advantage to 4-PPM when making comparisons. Using the peak optical power, the *Q*-factor for OOK and 2, 4-PPM will be similar in the absence of turbulence. However, PPM with SDD is expected to offer lower error probability

especially in the presence of turbulence. A similar result is expected between BPSK and PPM-BPSK. The argument will be clear when the *Q*-factor and error probability are compared among different modulation schemes.

Fig. 2 shows the received OOK-NRZ signal transmitted at the rate of 1 Mbps in the presence of turbulence with σ_I^2 =0.54. The severity of the turbulence effect clearly shows that a fixed threshold will not be able to recover the binary data (note that the optical signal is non-negative, however due to a coupling capacitor at the output of the receiver, the electrical signal is bipolar).

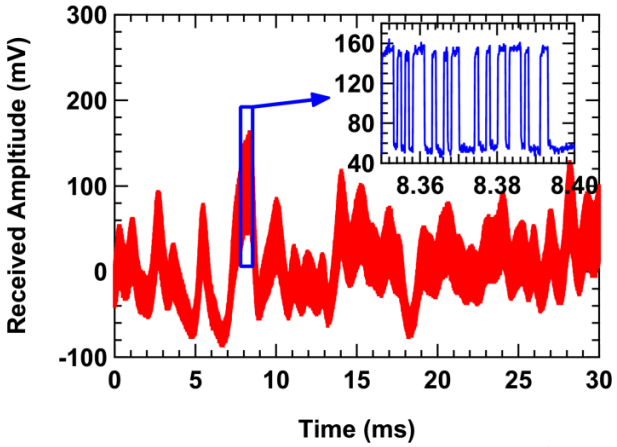

Fig. 2 Received OOK-NRZ signal at 1 Mbps in the presence of turbulence (SI = 0.54).

The severe effect of turbulence in OOK-NRZ is further demonstrated in Fig. 3(a), which shows the received amplitude histograms for the turbulence (black) and turbulence free (red) channels. The histogram clearly shows the data can be decoded without any errors for the non-turbulent channel using a fixed threshold value. However, the histogram in the presence of turbulence shows that there is no clear threshold level, and an error free link cannot be achieved using a fixed threshold. Comparing the histogram of BPSK (Fig. 3(b)) in similar conditions show that BPSK offers substantial resilience to turbulence. Though the signal variance of BPSK in the presence of turbulence is higher than without the turbulence case (represented by the wider peaks in the histogram), the threshold level is still clear, demonstrating a lower error probability.

The *Q*-factor and SER of OOK, BPSK, 2, 4-PPM and 2-, 4-PPM-BPSK against the SI is given in Fig. 4 (a) and (b), respectively. As discussed above, the peak transmitted optical power of PPM and OOK are made equal in order to make the *Q*-factor in the absence of turbulence equal, which is verified in Fig. 4(a). Note that the *Q*-factors for OOK and PPM are almost identical in the presence of the turbulence as well, as these are both amplitude based modulation formats. On the other hand, the *Q*-factors of SIM based modulations (BPSK and PPM-BPSK) are ~3 dB less than OOK at $\sigma_I^2 = 0$.

Recalling that BPSK requires an additional 1.5 dB optical power for the same signal-to-noise ratio, this is expected. However, the *Q*-factor in the presence of turbulence is significantly higher than OOK and PPM, as the information is encoded into the phase of the RF sub-carrier. The SER curve Fig. 4(b) shows the susceptibility of OOK to turbulence, as the error rate increased from less than 10^{-6} to 10^{-4} at σ_I^2 of 0.1. A similar error profile was shown by PPM with HDD (not shown in the figure for clarity). The PPM with SDD offers remarkable resilience to turbulence as the SER is less than 10^{-6} at $\sigma_I^2$of 0.58. The BPSK and PPM-BPSK also demonstrate improved performance in a turbulence channel with an error rate less than 10^{-6} at $\sigma_I^2$of 0.4 for BPSK. PPM-BPSK with HDD also displays a similar SER profile (not shown in the figure for clarity). Finally, PPM-BPSK with SDD offered improved performance in comparison to BPSK. The best performance is offered by PPM with SDD. Since the average transmitted power for 4-PPM is half that of other schemes, a further improvement can be expected if the average transmit power was made same.

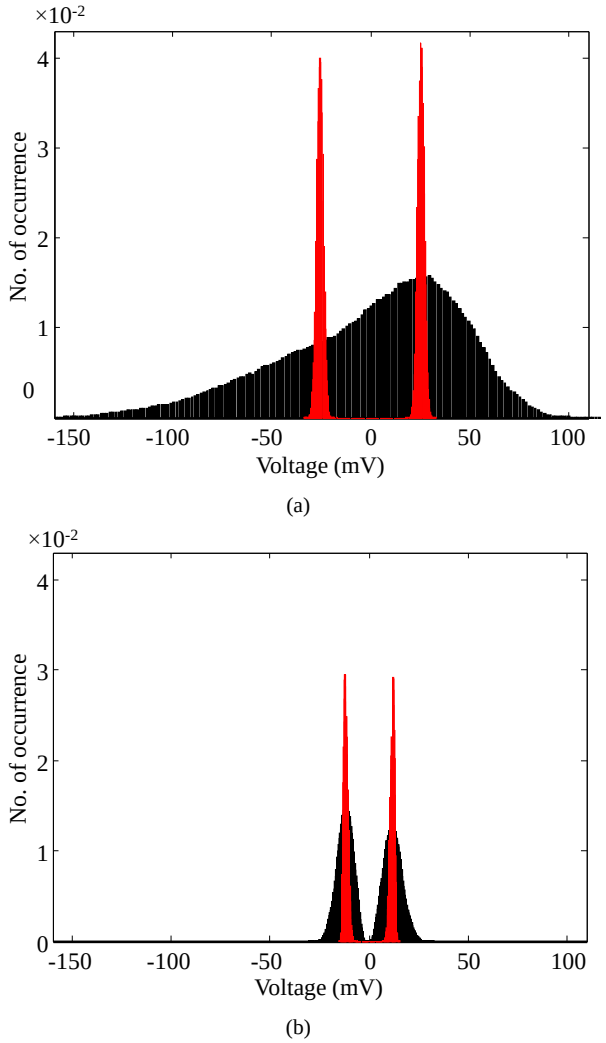

Fig. 3 The histogram of the 1 Mb/s received signal with (blue, σ_I^2 = 0.54) and without (red) turbulence for: (a) OOK-NRZ, and (b) BPSK. Note that the total number of occurrences is normalized to 1 for clarity of figures.

Experiments were carried out for different transmit optical powers for verification of the results. The *Q*-factors and SERs in the presence and absence of turbulence at a reduced transmit power (18 mV received peak-to-peak voltage) are shown in Fig. 5. As in the previous cases, the *Q*-factor profiles for OOK and PPM, and BPSK and PPM-BPSK are similar.

The SER curves verify the previous results that 4-PPM with SDD offer the best performance of all modulation schemes. However, the SER is higher than 10^{-6} at an SI of 0.15. This is due to the reduced transmit optical power.

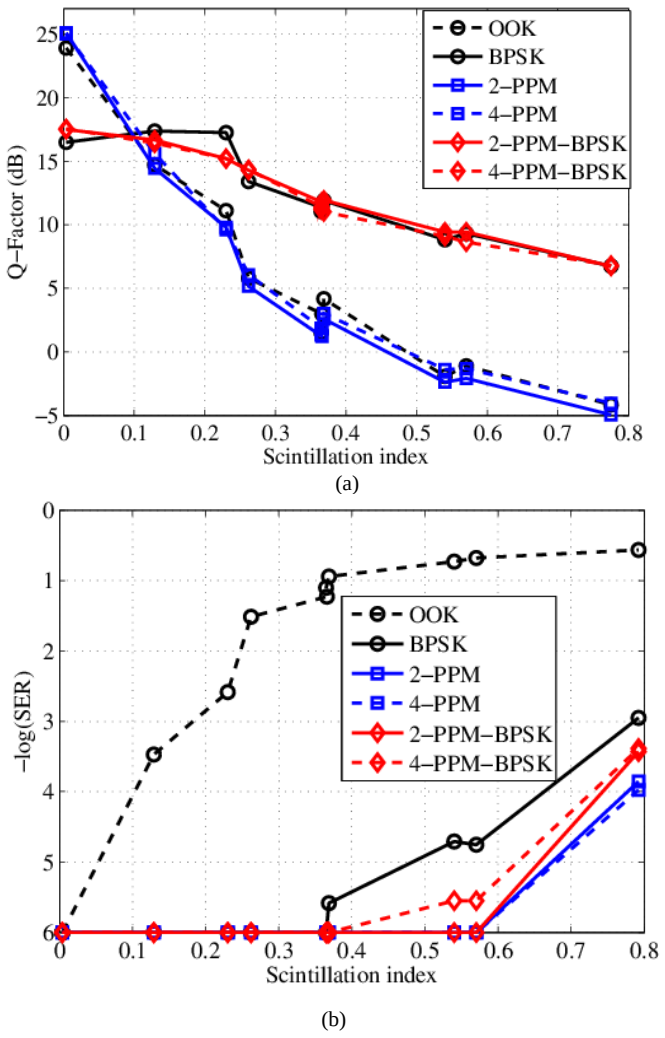

Fig. 4 The measured (a) *Q*-factor, and (b) error probability against different SI for different modulation schemes for received peak-to-peak voltage of 52mV.

The results shown clearly establish the superior robustness of the PPM scheme in comparison to other modulations in a weak turbulence channel. The significantly improved performance of 2, 4-PPM, in comparison to OOK, make them more suitable for outdoor FSO links. The results obtained closely match with simulation and theoretical predicted data, as given in [9], where it was established that PPM offers the best performance followed by PPM-BPSK for the $\sigma_I^2 < 0.5$. It was observed that PPM offers marginally superior error performance in comparison to BPSK even at higher values of σ_I^2. This is attributed to the unavoidable synchronization issue in PPM-BPSK especially in the presence of turbulence. Theoretical analysis was carried out assuming perfect synchronization, which is rather challenging to achieve experimentally.

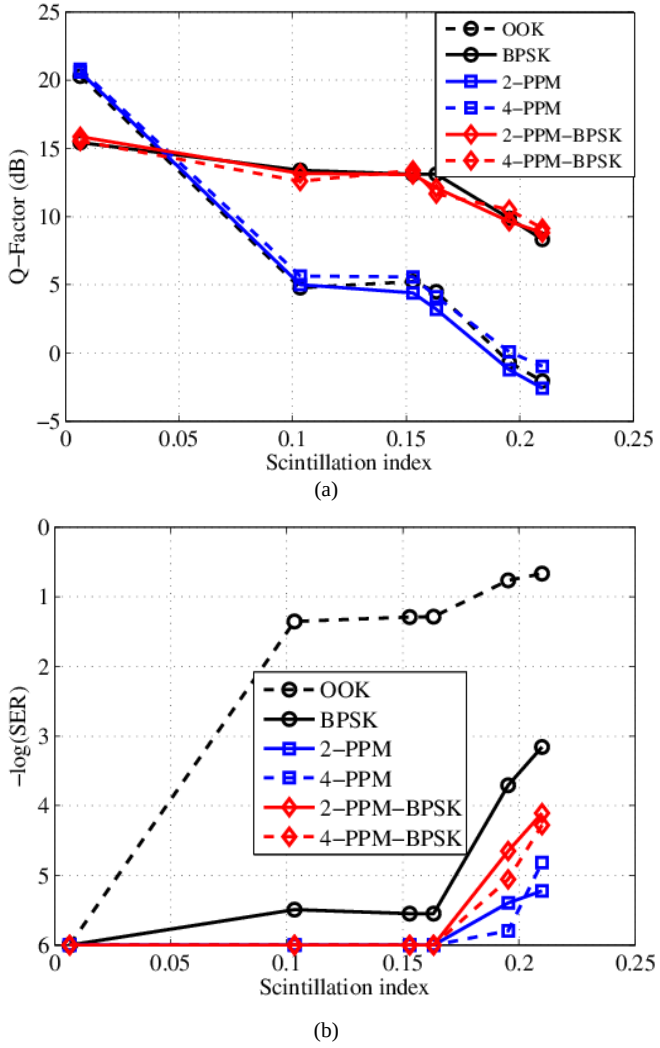

Fig. 5 The measured (a) *Q*-factor, and (b) error probability against different SI for different modulation schemes for received peak-to-peak voltage of 18mV.

IV. Conclusion

In this paper, experimental evaluation of error performance for different modulation schemes for FSO communication links in a turbulence channel was reported. The turbulence was created by introducing hot and cold air in an indoor atmospheric chamber and the temperature profile along the propagation path was measured to characterize the channel. The strength of turbulence was classified as weak based on the measured scintillation index. The *Q*-factors as well as the slot error rates for different modulation schemes were measured for different turbulence regimes. The measured error rate showed that OOK with a fixed threshold decoding level offered the worst performance while PPM with soft decision decoding offered the best performance among the modulation schemes studied followed by PPM-BPSK. These results clearly demonstrated the effectiveness of PPM to overcome high random fading in the turbulence environment.

V. Acknowledgment

The project was supported by the EU FP7 COST ACTION IC1101.

References

[1] M. Grabner and V. Kvicera, "Multiple scattering in rain and fog on free-space optical links," *Journal of Lightwave Technology*, vol. 32, pp. 513-520, 2014.

[2] Z. Ghassemlooy, W. O. Popoola, and S. Rajbhandari, *Optical Wireless Communications – System and Channel Modelling with Matlab*, 1st ed.: CRC Press, 2012.

[3] X. Zhu and J. M. Kahn, "Mitigation of turbulence-induced scintillation noise in free-space optical links using temporal-domain detection techniques " *IEEE Photonics Technology Letters*, vol. 15, pp. 623-625, 2003.

[4] W. Gappmair, "Further results on the capacity of free-space optical channels in turbulent atmosphere," *IET Communications*, vol. 5, pp. 1262-1267, 2011.

[5] W. O. Popoola and Z. Ghassemlooy, "BPSK subcarrier intensity modulated free-space optical communications in atmospheric turbulence," *Journal of Lightwave Technology*, vol. 27, pp. 967-973, 2009.

[6] J. Li, J. Q. Liu, and D. P. Taylor, "Optical communication using subcarrier PSK intensity modulation through atmospheric turbulence channels," *IEEE Transaction on Communications*, vol. 55, pp. 1598-1606, Aug. 2007.

[7] C. C. Davis and I. I. Smolyaninov, "Effect of atmospheric turbulence on bit-error rate in an on-off-keyed optical wireless system," in *Proc. SPIE* 2002, pp. 126-137.

[8] F. Xu, M. A. Khalighi, and S. Bourennane, "Pulse position modulation for FSO systems: Capacity and channel coding," in *Telecommunications, 2009. ConTEL 2009. 10th International Conference on*, 2009, pp. 31-38.

[9] M. Faridzadeh, A. Gholami, Z. Ghassemlooy, and S. Rajbhandari, "Hybrid pulse position modulation and binary phase shift keying subcarrier intensity modulation for free space optics in a weak and saturated turbulence channel," *Journal of the Optical Society of America A*, vol. 29, pp. 1680-1685, 2012/08/01 2012.

[10] W. Gappmair, S. Hranilovic, and E. Leitgeb, "Performance of PPM on terrestrial FSO links with turbulence and pointing errors," *Communications Letters, IEEE*, vol. 14, pp. 468-470, 2010.

[11] S. Xuegui, Y. Fan, and J. Cheng, "Subcarrier intensity modulated optical wireless communications in atmospheric turbulence with pointing errors," *Optical Communications and Networking, IEEE/OSA Journal of*, vol. 5, pp. 349-358, 2013.

[12] Z. Ghassemlooy, H. Le Minh, S. Rajbhandari, J. Perez, and M. Ijaz, "Performance analysis of Ethernet/fast-Ethernet free space optical communications in a controlled weak turbulence condition," *Journal of Lightwave Technology*, vol. 30, pp. 2188-2194, 2012.

[13] W. Hirt, M. Hassner, and N. Heise, "IrDA-VFIr(16Mbits/s): Modulation code and system design," *IEEE Personal Communications* vol. 8, pp. 58 - 71, 2001.

[14] S. Rajbhandari, P. A. Haigh, Z. Ghassemlooy, and W. Popoola, "Wavelet-neural network VLC receiver in the presence of artificial light interference," *IEEE Photonics Technology letters*, vol. 25, pp. 1424-1427, 2013.

[15] L. C. Andrews and R. L. Phillips, *Laser beam propagation through random media*, second ed. Washington: SPIE Press, 2005.

[16] G. R. Osche, *Optical Detection Theory for Laser Applications*, 1 ed.: Wiley-Interscience, 2002.

[17] X. Song and J. Cheng, "Subcarrier intensity modulated optical wireless communications using noncoherent and differentially coherent modulations," *Journal of Lightwave Technology*, vol. 31, pp. 1906-1913, 2013.

[18] A. K. Majumdar and J. C. Ricklin, *Free-Space Laser Communications: Principles and Advances*. New York: Springer, 2008.

[19] A. R. Hayes, "Digital pulse interval modulation for indoor optical wireless communication systems," Phd Sheffield Hallam University, UK, 2002.